Contents

Network Modeling and Planning for Fixed Wireless Access Applications

Brecht De Beelde*, Mike Vantorre, German Castellanos, Mario Pickavet, Wout Joseph

Department of Information Technology, Ghent University/IMEC, 9052 Ghent, Belgium

Abstract

The large bandwidths that are available at millimeter wave frequencies enable fixed wireless access (FWA) applications, in which fixed point-to-point wireless links are used to provide internet connectivity. In FWA networks, a wireless mesh is created and data is routed from the customer premises equipment (CPE) towards the point of presence (POP) which is the interface with the wired internet infrastructure. The performance of the wireless links depends on the radio propagation characteristics, i.e., the environment, and it depends on the wireless technology that is used. In this work, we analyze the network characteristics of FWA networks using radio propagation models for different wireless technologies and scenarios, for frequencies 28 GHz, 60 GHz, and 140 GHz. The influence of rain, vegetation, number of subscribers, and the environment is considered. A network planning algorithm is presented that defines a route for each CPE toward the POP, based on a predefined location of customer devices, and considering the available capacity of the wireless links.

Keywords: Fixed wireless access, FWA, mmWave, network design, routing algorithm, graphs.

2022 MSC: 00-01, 99-00

*Corresponding author

Email address: Brecht.DeBeelde@UGent.be (Brecht De Beelde)

URL: http://waves.intec.ugent.be/ (Brecht De Beelde)

1. Introduction

During the past decade, the need for broadband connectivity has increased. Not only do end-users require more data volumes and higher data rates, e.g., for online gaming and video-on-demand streaming services, but also the data volumes of enterprises have risen, e.g., due to digitalization, video conferencing, and telework [1]. As the capacity of the current wired infrastructure is limited, e.g., the data rate that can be obtained using digital subscriber line (DSL) technology is generally limited to 100 Mbps [2], network operators are required to update their access networks to enable broadband networks. Fiber optic cables offer download speeds up to 10 Gbps [3] but have a high installation cost [4]. In fixed wireless access (FWA) applications, the last mile of the access network is replaced by a wireless link using a point-to-point radio network. The large bandwidths that are available at millimeter wave (mmWave) frequencies enable broadband access networks [5] with a lower installation cost compared to the deployment of a fiber network, as no costly digging is required [4].

In this paper, we characterize FWA networks via graph analysis using state-of-the-art radio propagation models, and we present a tool to perform network planning of FWA networks. Different scenarios and environments are considered, and network capacity calculations are performed for different wireless technologies envisioned for FWA networks, i.e., fifth-generation (5G) communication in the 28 GHz band, and IEEE Std. 802.11ad in the 60 GHz band. We also perform capacity calculations for the 140 GHz band that is envisioned for future wireless communication systems.

The outline of this paper is as follows. We start by describing the FWA network architecture and a presentation of related research. In Section 2, we provide an overview of the different radio propagation models that are used in this work, followed by the methodology of how the network analysis and planning are performed. We also present how network data is obtained via simulations to model an FWA network. In Section 3, the FWA network analysis is presented, and Section 4 presents the network planning results. Section 5

concludes this paper. The implementation details of the network modeling and planning tool are discussed in the Appendix.

1.1. Fixed wireless access background

In FWA networks, internet connectivity is provided to residential and enterprise buildings via fixed wireless links, i.e., static wireless links are set up between multiple wireless devices [6]. In the network, different types of devices exist. Customer premises equipment (CPE) devices bridge the FWA network to the local area network (LAN) of the user. They are typically connected at building facades above street level to limit attenuation due to moving people and cars. A point of presence (POP) device is the interface of the FWA network with the wired (backbone) infrastructure. Therefore, all CPE devices need to be able to connect to a POP device in order to be connected to the network. There can be multiple POP devices, which increases the FWA network robustness. However, most CPE devices won't be able to connect to a POP device directly. Instead, a wireless mesh network is created which enables a connection from each CPE in the network towards a POP. The number and location of CPE devices depend on the customers that subscribe to the FWA network and cannot be controlled by the network operator. In most cases, the location of the POP is also predefined, e.g., based on the available wired backbone infrastructure. It is possible that, given predefined CPE and POP locations, some CPE devices are not connected to a POP, because they have no neighboring devices to which they can connect, or because the capacity of some wireless links is not sufficient to transfer the data of all CPEs that use the link. To create a mesh network where all CPE devices get connected to a POP device, EDGE devices might be added to the FWA network. They can be installed on public buildings or street furniture, including lampposts and street signs, and do not directly connect a customer to the network. Instead, they enable connectivity of CPE devices and increase network capacity.

Work on standardization of broadband wireless access systems started two decades ago and resulted in IEEE Std. 802.16 that specifies the air interface,

including the medium access control layer (MAC) and physical layer (PHY) of fixed and mobile point-to-multipoint broadband wireless access systems [7]. The IEEE Std. 802.16 considers frequencies ranging from 10 GHz to 66 GHz, using channel bandwidths of 25 MHz, which is 5 times more than the bandwidth of long-term evolution (LTE) channels. The maximum data rate of an IEEE Std. 802.16 link is 120 Mbps, which is 5 times the data rate of 24.4 Mbps for a single-input single-output (SISO) LTE system with quadrature amplitude modulation (256-QAM) and which follows the Shannon capacity theorem. Recent advancements in radio technology have realized mmWave radio communication for frequencies up to 100 GHz [8, 9], and enable high-throughput wireless communication systems. Furthermore, the small wavelengths allow large antenna arrays resulting in highly directive antennas and facilitating beamforming. The IEEE Std. 802.11ad specifies PHY and MAC layer interfaces for short-range high-throughput wireless systems with carrier frequencies in the V-band (50-75 GHz) and channel bandwidths of 2 GHz, allowing SISO data rates up to 4.6 Gbps [10]. Its successor IEEE Std. 802.11ay supports multiple-input multiple-output (MIMO) systems and allows data rates up to 40 Gbps [11].

1.2. Related research

A tutorial on technologies and design considerations for FWA networks is provided in [6]. In [12], a mathematical model is presented for the automatic selection and configuration of base stations for FWA networks with wireless technologies using a carrier frequency of 3.5 GHz. FWA network design using 5G technology is discussed in [13], and beam alignment at mmWave frequencies is discussed in [14]. In [15], capacity and coverage calculations for FWA using 5G technology in the 3.5 GHz and 28 GHz bands are presented. A study on the probability of signal outage probabilities for wireless backhaul communication at 28 GHz and 73 GHz is presented in [16]. In [5], a propagation model is provided for suburban FWA networks at 28 GHz with 90% coverage. Outdoor channel models for FWA applications are presented in [17] for wireless technologies at 60 GHz and in [18] for 140 GHz. The use of IEEE Std. 802.11ay for FWA

networks is studied in [19]. Link budget calculations for FWA networks are presented in [20] for links using carrier frequencies ranging from 75 GHz to 400 GHz, and in [21] for frequencies from 300 GHz to 900 GHz.

1.3. Contributions

In this work, we present a study on FWA network characterization for different environments and scenarios. We consider frequency bands that are used in existing wireless technologies, i.e., the 28 GHz band used in 5G and the 60 GHz band used in IEEE Std. 802.11ad, as well as a frequency band at 140 GHz that could be used for future wireless communication systems. We use state-of-the-art radio propagation models to calculate the capacity of the wireless links for different scenarios. We also present a framework to analyze FWA network characteristics and to perform network planning. The framework is implemented in Python and uses graph theory to define the location of EDGE devices. It implements an algorithm that routes traffic from all CPE devices towards a POP, considering the available data rates on the wireless links.

2. Methodology

To characterize FWA networks using different technologies and considering different scenarios, propagation models and network data are required. We start in Section 2.1 with a presentation of the used radio propagation models, followed by a presentation of link budget calculations in Section 2.2. Section 2.3 presents how the FWA networks are characterized and Section 2.4 presents the network planning algorithm. We present in Section 2.5 how FWA network data is obtained via simulations, and conclude in Section 2.6 with a presentation of the considered scenarios for the network characterization and user requirements for the validation of the planning algorithm.

2.1. Radio propagation models

Radio propagation models characterize how electromagnetic waves propagate in a certain environment. They not only depend on the specific envi-

ronment, but also on the carrier frequency. In this work, we use propagation models for outdoor environments and we consider three frequency bands that are well suitable for FWA networks, i.e., the 5G mmWave band at 28 GHz, the mmWave industrial, scientific, and medical (ISM) band at 60 GHz, which is used in IEEE Std. 802.11ad, and a potential mmWave band for future wireless communication systems at 140 GHz.

In the following sections, different propagation mechanisms are discussed that influence FWA networks.

2.1.1. Path loss

Path loss is the signal attenuation between a transmitting and receiving antenna, due to the spherical expansion of a waveform. In a free space environment, the electromagnetic wave does not interact with any objects, and the path loss depends on the distance, as well as the carrier frequency of the wireless technology. Path loss PL (in dB) in a free space environment is calculated via (1), with f the frequency (in Hz), d the distance (in meter), and c the speed of light in air, i.e., c = 3e8 m/s.

$$\mathrm{PL}(f,d) = 20\ \log_{10}\left(4\pi d\frac{f}{\mathrm{c}}\right) \tag{1}$$

Path loss increases with distance and with frequency. For a link with a distance of 100 m, path loss in free space is 101.4 dB at 28 GHz, 108.0 dB at 60 GHz, and 115.4 dB at 140 GHz. In realistic environments, object interactions may occur, and path loss is often modeled using empirical channel models, e.g., using the one-slope model from (2), with PL_0 the reference path loss in dB at distance d_0, and n the dimensionless path loss exponent that defines the distance dependence. The shadow margin χ_σ is based on a normal distribution with standard deviation σ in dB.

$$\mathrm{PL}(f,d) = \mathrm{PL}_0(f,\mathrm{d}_0) + 10\mathrm{n}\log_{10}\left(\frac{d}{\mathrm{d}_0}\right) + \chi_\sigma \tag{2}$$

The model parameters PL_0, n, and σ are fitted based on measurement data. In Line-of-Sight (LOS) scenarios, no objects are present in the first Fresnel

Table 1: One-slope path loss model parameters for different frequencies.

Frequency	PL_0	n	σ	Reference
28 GHz	61.4 dB	2.1	3.6 dB	[22]
60 GHz	71.0 dB	1.8	2.9 dB	[17]
140 GHz	75.9 dB	1.9	1.4 dB	[18]

zone of the link between the two antennas and the direct path is unobstructed. The fitted parameters for LOS scenarios at different frequencies are presented in Table 1 At mmWave frequencies, limited interactions occur, and the fitted parameters are close to the free space scenario. Due to the highly directive antennas used in FWA systems, free space path loss is a good representation in case of an unobstructed Line-of-Sight path [22, 17, 18].

2.1.2. Atmospheric absorption

Radio waves at mmWave frequencies do not only attenuate due to the spreading of the wavefront, attenuation is also caused by absorption by atmospheric gasses, i.e., oxygen and water vapor molecules [23]. As the gaseous component has a set of spectral absorption lines, the atmospheric attenuation is frequency-dependent [24].

In this work, the International Telecommunication Union (ITU) recommendation on attenuation by atmospheric gases and related effects is used to obtain attenuation values for the different frequency bands [25]. The specific attenuation in dB/km is predicted for an air pressure of 1.013,25 hPa, a temperature of 15°C, and a water vapor density of 7.5 g/m^3. A visualization of the attenuation at sea level is shown in Fig. 1, from which we conclude there is a peak in attenuation at 60 GHz, with a specific attenuation of 20 dB/km [26]. At 28 GHz (0.06 dB/km) and 140 GHz (0.4 dB/km), the attenuation is limited.

The one-slope PL model parameters from Table 1 include the atmospheric absorption, but the effect of the atmospheric absorption is limited due to the

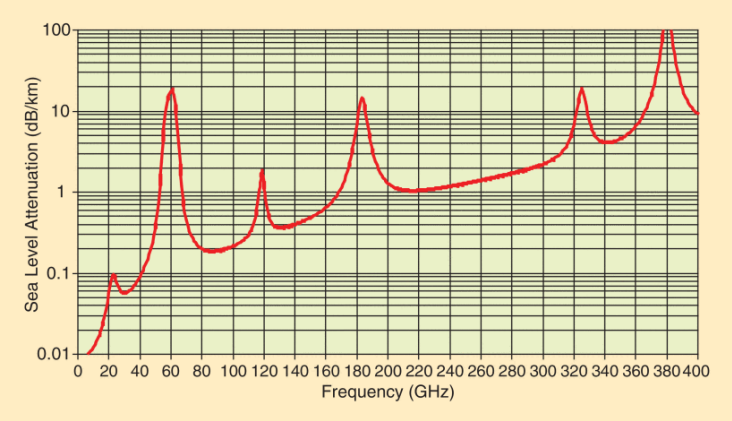

Figure 1: Atmospheric absorption for frequencies up to 400 GHz [26].

relatively small antenna separations, up to 130 m, during the measurements.

2.1.3. Rain attenuation

The wavelengths corresponding to mmWave frequencies range from 10.7 mm at 28 GHz to 1 mm at 300 GHz, while the diameter of raindrops is on the order of 1 to 10 mm. Therefore, electromagnetic waves incident on raindrops will suffer from attenuation and scattering, in addition to the permittivity of water which also differs from free space [27]. As such, the received signal strength will decrease in the event of rain, causing a lower link capacity.

Multiple models are available to predict attenuation due to rain [27, 28, 29]. We use the recommendation from the ITU which predicts the specific attenuation γ in dB/km via (3), with R the rain rate in mm/h and k and α frequency-dependent coefficients that are derived via a scattering analysis [30].

$$\gamma = kR^{\alpha} \tag{3}$$

Table 2 presents the specific attenuation for two rain rate intensities at different frequencies. The specific attenuation for a rain rate of 25 mm/h ranges from 3.9 dB/km at 28 GHz, up to 6.8 dB/km at 60 GHz and 12.6 dB/km at 140 GHz.

Table 2: Specific attenuation in dB/km for two rain rate intensities at frequencies 28 GHz, 60 GHz, and 140 GHz.

Rain rate	28 GHz	60 GHz	140 GHz
15 mm/h	2.4 dB/km	6.8 dB/km	9.0 dB/km
25 mm/h	3.9 dB/km	9.5 dB/km	12.6 dB/km

2.1.4. Vegetation loss

In FWA networks, antennas are mounted at the building facades and above street level, to limit link obstructions by vehicles and other objects. However, it is possible that trees obstruct the LOS path between two devices. Therefore, we need to take into account the attenuation due to vegetation obstructing the wireless link.

Multiple models are available to estimate vegetation loss as a function of frequency and vegetation depth [31, 32, 33, 34, 35]. These models have the generic form of (4), with f the frequency in MHz or GHz and d the vegetation depth in meters. Model parameters A, B, and C are estimated from measurement data.

$$\mathrm{L}(f, d)[\mathrm{dB}] = \mathrm{A} f^{\mathrm{B}} d^{\mathrm{C}} \tag{4}$$

The Weissberger [31] and ITU-R [32] models are applicable for frequencies up to 95 GHz. The COST-235 model [33] is applicable for frequencies up to 57 GHz, and the FITU-R model [36] is applicable up to 40 GHz. In [37], the COST-235 model provides the best fit to measured vegetation loss at 60 GHz. Parameter B of the COST-235 model has a negative value of -0.009, and the vegetation loss decreases with increasing frequency, as the smaller Fresnel radius at higher frequencies allows radio propagation via the gaps in the vegetation [34]. The vegetation-dependent exponential decay (VED) model from [34] takes the vegetation density into account and is applicable for frequencies in the D-band, which includes 140 GHz.

For the remainder of this paper, the COST-235 model is used at frequencies

28 GHz and 60 GHz, and the VED model is used at frequency 140 GHz. The estimated vegetation loss for a vegetation depth of 10 m are 25.9 dB at 28 GHz, 25.7 dB at 60 GHz, and 15.2 dB at 140 GHz.

2.2. Link budget calculation

A link budget calculation allows determining the maximum data rate and range of a wireless system. It is based on configuration parameters, including the used wireless technology and antenna characteristics, as well as the propagation model. We calculate the received power (P_R) in dBm of the electromagnetic wave using the link budget equation presented in (5), in which P_T is the transmit power in dBm, G_T and G_R are the antenna gains in dBi of the transmitting and receiving antenna systems (including the array gain), L_T is the feeder loss in dB at the transmitting device, L_R is the loss in dB at the receiving device, and PL is the path loss in dB which includes environmental and atmospheric losses.

$$P_R = P_T + G_T + G_R - L_T - L_R - PL \tag{5}$$

With higher received powers, more complex modulation and coding schemes (MCS) can be used, resulting in higher throughputs. The receiver sensitivity P_{RS} (in dBm) is the minimum received power that is required to use a certain MCS, and it depends on the wireless technology and on the used MCS. The received power should be higher than the receiver sensitivity to use a certain MCS and to achieve the corresponding data rate.

The IEEE Std. 802.11ad specification [10] lists the minimum receiver sensitivities for the different MCS, ranging from P_{RS} = -68 dBm for MCS 1 that enables a maximum data rate of 385 Mbps, up to P_{RS} = -53 dBm for MCS 12 that has a data rate of 4.62 Gbps, using a single carrier physical layer.

2.3. Network analysis

We use graph theory to analyze FWA networks. We have analyzed the following metrics for the different networks.

Average cpe vertex degree $\delta_{\mathbf{v,avg}}$: The average number of links of all CPE devices

POP eccentricity $\epsilon_{\mathbf{POP}}$: Maximum of the shortest distance from the POP to all other CPE devices in the graph

Median link length $\mathbf{d_{med}}$: Median distance in meters between two devices

Average path length $\mathbf{l_{avg}}$: Average hop count of the shortest path length of all CPE devices towards a POP device

Total network capacity $\mathbf{c_{avg}}$: The total capacity of the network that is available on all wireless links

These metrics influence the performance of the network. With a higher average CPE vertex degree, the network density increases. With more possible links between devices, the total network capacity increases, and fewer EDGE devices are required to get a route from each CPE device towards a POP device. The average path length also gives an indication of the network capacity, as wireless links with a smaller link distance have a higher capacity. The average path length, measured in hop count, influences the network performance on a higher level. As radio propagation in free space travels at the speed of light, propagation delays are minimal. However, with a higher number of hops on the path, the packet latency will increase due to an increased processing time on the hops. Therefore, the latency in dense networks is expected to be smaller than for the field trial and early adopters scenarios.

The analysis is done using Python's igraph package, and the validation of our analysis scripts is performed using a simplified small FWA network for which we can easily calculate graph statistics manually. The results of the network analysis are presented in Section 3.

2.4. Network planning

The goal of the network planning algorithm is twofold. First, the locations of EDGE devices need to be defined in order to get all CPE devices connected to the

FWA network. Second, each CPE device needs to have a route with sufficient capacity towards a POP device. EDGE devices do not connect any customers directly and are added to the network for two reasons. First, they can be used to create a wireless mesh, i.e., connect CPE devices that can otherwise not connect to the FWA network. Second, they increase the network capacity, e.g., when the capacity of a wireless link is not sufficient to transfer the required data.

During the network planning phase, a route is defined for each CPE towards a POP, given all CPE and POP device locations, and a predefined quality of service (QoS) requirement, i.e., we need to allocate a certain data rate for each CPE on the wireless links that are used to reach the POP device.

2.4.1. Prerequisites

The required input data for the network planning algorithm is a database containing the LOS links between all devices as well as the link distances in meters. The link budget parameters from Section 2.2 are configured, including a constant antenna gain (independent of the beamforming angle), the rain rate, and possible vegetation obstructing the LOS path. No reflected paths are considered. Furthermore, each CPE device has an associated data rate requirement. In Section 2.5, the methodology is described how the database with wireless link info is obtained.

2.4.2. Preparation

From the database, a graph is constructed where vertices represent devices, with device type (CPE, POP, or EDGE), data rate requirement (for CPE devices), and physical location as attributes. In the graph, edges represent that a LOS path is present between two devices, with the distance (in meters) as an attribute. From the distance attributes, wireless link capacities are calculated based on the link budget calculation presented in Section 2.2 and added as an additional attribute. One additional (artificial) POP device is added, which is connected to all other POP devices. This allows network topologies with multi-

ple POP devices. The capacity of a link connecting a POP device to the artificial parent POP is the sum of all capacities of the child POP device.

Feasibility checks are performed on the input data before running the network planning algorithm. A first check consists of verifying that the input graph is connected, i.e., there is a path from any vertex to any other vertex in the graph. If not, it is impossible to serve the unconnected CPE devices as no path towards a POP exists. A second feasibility check consists of summing the required data rates of all CPE devices and verifying that this is smaller than the sum of capacities of the links towards the artificial parent POP. If this is not the case, there is a capacity constraint at the POP devices and not all CPE devices will have their required data rate at peak moments. If one of these feasibility checks fails, a manual interaction is required during which EDGE devices are added to the network, as we will describe in the next section. This manual interaction in network planning is also required to apply with (local) regulations [38]. If the capacity of the wireless links of the POP is not sufficient, additional EDGE devices can be added near the POP device, or additional POP devices can be added. This is again a manual decision, based on the available infrastructure.

2.4.3. Algorithm

Algorithm 1 describes the network planning algorithm, based on an input graph with vertices that represent CPE, EDGE, and POP devices, and edges that represent LOS links between devices. In the first step, the CPE devices are sorted. For all vertices with a CPE type attribute, the shortest paths towards the artificial POP are calculated via Dijkstra's algorithm [39], using link distances as weights. The vertices are sorted in the following order:

1. The required data rate
2. The number of shortest paths
3. The number of hops on the shortest path

We first perform routing for the vertices with the highest data rate requirement, to prevent that we first optimize routes of other vertices and have no more link

Data: Input graph g

Result: A route to a POP device for each CPE device

for *all vertices v with* CPE *device type in g* **do**

    Obtain the data rate requirement dr from v;

    Define the number of shortest paths n from v to POP (Dijkstra);

    Define the number of hops h on the shortest path ;

end

Sort all vertices based on dr, n, and h ;

for *all vertices v (sorted) g* **do**

    Create local copy g' of g ;

    Define shortest path p from v to POP (Dijkstra);

    while *p in g' contains edge e with insufficient capacity* **do**

        Remove e from g';

        Get shortest path p in g' from v to POP;

        if *No shortest path found* **then**

            Print error message: Manual interaction required ;

            Move to next vertex ;

        end

    end

    Add an attribute to v with path info p;

    Subtract dr from all edge throughput attributes;

    if *available throughput attribute of edge smaller than minimum network throughput* **then**

        Remove e ;

    end

end

Algorithm 1: Network routing for predefined throughput requirements

capacity available to serve the high-demanding customers. For vertices with identical data rate requirements, routing is first performed for vertices with the lowest number of shortest paths towards the (parent) POP device. Lastly, for vertices with equal data rate requirements and number of shortest paths, we perform routing first for the vertices with the highest number of hops on the shortest path.

After having a sorted list of vertices for which we need to define routing towards the POP device, we again use the shortest path algorithm to define the routing. An attribute is added to the vertex with the path that needs to be followed, and the available link capacity attribute is updated on all edges along that path, i.e., the "available" remaining data rate of the wireless link is lowered by the throughput requirement of the vertex. If the available data rate on an edge is lower than the data rate requirement of the network, we run the shortest path algorithm again after temporarily removing the edge from the graph. If the available data rate on an edge is lower than the minimum data rate requirement of the network, we remove the edge to prevent that this edge will be used for routing traffic of other vertices. Therefore, the graph gets updated and the shortest path algorithm will result in other paths compared to the first time we ran the algorithm.

If the preparation or network planning has failed, e.g., due to the graph non-connectivity or due to a throughput bottleneck on one of the wireless links, a manual intervention is required, in which additional EDGE devices are placed in the network. The determination of the location of the EDGE devices is a manual task that is difficult to automate, due to the high number of legal and practical restrictions where EDGE devices might be placed, i.e., the placement of base stations is subject to regulations [40]. Furthermore, the number of EDGE devices in the network is expected to be limited. The locations of the additional EDGE devices are added to the input database, as well as the LOS links, and their corresponding distances, to other devices in the network.

The algorithm is implemented in Python. A presentation of the network characterization and network planning tool is provided in the Appendix.

2.5. Network data acquisition

We obtain FWA network data from simulations using the green radio access network design (GRAND) tool which is a deployment tool for wireless radio access networks [41]. The tool is designed for network planning of cellular networks, i.e., to define base station locations considering mobile users, and has been adjusted to enable the simulation of FWA networks [42].

The starting point of the tool is a map of the considered deployment environment. The map consists of three parts: the building locations, the street locations, and the area limits. All the buildings get a unique building identifier. In Belgium, this map is freely available from the government or from OpenStreetMap [43]. A configurable number of CPE devices are added to this map, with the constraints that there can be at most one device per building and that the device is positioned at the building's facade near the street. The Cartesian coordinates of these devices are randomly defined via a uniform distribution using the area limits from the map. For each device, new coordinates are generated as long as the coordinates do not correspond with a building that does not already have a node. Once the coordinates correspond to a building, they are modified so that the node is located at the street-level facade of the building at a height of 4 m above the ground. The result of the CPE device placement algorithm is that a predefined number of nodes are randomly allocated to different buildings on the map, at the facade closest to the nearest street. From the GRAND tool, we get a database with identifiers and coordinates of all CPE devices. In the second step, the possible radio links between different CPE devices are defined, by searching for possible LOS paths between two devices, based on the location of devices and the map with building locations. From this second step, we get a database with all LOS links between the different CPE devices. For each link, we get the identifiers of the two devices, as well as the link distance in meters.

By selecting different input maps, network data for different environments is generated. By adjusting the number of CPE devices that are present in the network, different scenarios are simulated.

2.6. Considered scenarios

In this paper, we consider the scenarios for different FWA networks listed in Table 3. For each scenario, we run 50 simulations with the GRAND tool to consider the randomness of the scenarios. Each simulation results in a database with CPE device locations and all the LOS links between the devices. Three environments are compared, each having a surface area of 1 km^2: downtown Ghent as an urban city, Leest as an urban village, and a rural area in the neighborhood of Leest. The environments are shown in Fig. 2. The number of CPE devices in the area, i.e., the internet subscribers to the network, ranges from 50 to 600. For the rural environment, only 10 and 50 CPE devices are considered, as there are fewer than 100 buildings. In the centralized POP scenario, one POP

Table 3: Considered scenarios for FWA network analysis.

Parameter	Scenarios
Surface area	1 km^2
Number of CPE devices	50 (field trial network)
	100 (early adopters)
	300 (early majority)
	600 (late majority)
Number of POP devices	1 (central POP)
	3 (decentralized POP)
Environment	urban city (Ghent)
	urban village (Leest)
	rural (Leest)
Weather condition	sunny (no rain)
	rain (15 mm/h)
	heavy rain (25 mm/h)
Vegetation obstruction	none
	10% of the link is covered by vegetation

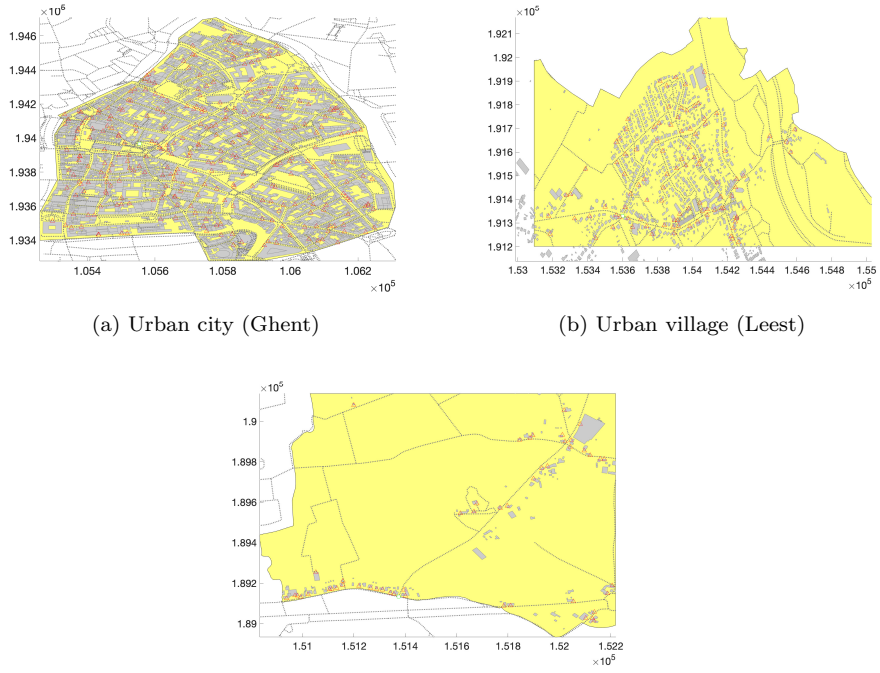

(a) Urban city (Ghent)

(b) Urban village (Leest)

(c) Rural (Leest)

Figure 2: Simulation environments for FWA network characterization, with gray surfaces representing the buildings, dashed lines representing the roads, red triangles representing simulated customer premises equipment (CPE) locations, a green square representing the fiber point of presence (POP), and the considered surface area shown in yellow.

device is located centrally at a location where a cabinet currently exists. In the decentralized POP scenarios, two random CPE devices are replaced by a POP device. The weather condition changes from sunny to heavy rain with a rain rate of 25 mm/h, and the influence of vegetation is analyzed assuming that 10% of the link distance is covered by vegetation.

For the user requirements, the two use cases presented in Table 4 are considered. In the first use case, it is assumed that all customers require a peak data rate of 300 Mbps. In the second use case, it is assumed that 30% of the customers subscribe to an economy plan (with a data rate of 30 Mbps), 30% of

Table 4: Considered throughput requirements of the network subscribers.

Use case	30 Mbps	100 Mbps	300 Mbps	500 Mbps
1	0%	0%	100%	0%
2	30%	30%	30%	10%

the customers subscribe to the standard plan (with a data rate of 100 Mbps), and 10% of the customers need a peak data rate of 500 Mbps.

Three different wireless communication technologies are considered: mmWave 5G at 28 GHz, IEEE Std. 802.11ad at 60 GHz, and then a future wireless communication system at 140 GHz. MmWave 5G operates from 26.5 GHz to 29.5 GHz and supports channel bandwidths up to 400 MHz. Using a 1/3 code rate, the minimum signal-to-noise ratio (SNR) ranges from 2.2 dB for binary phase shift keying (BPSK) modulation up to 25.2 dB for 256-QAM [44]. The maximum data rates that can be achieved are calculated via (6), with DR the data rate in Mbps, Q the modulation order that depends on the MCS, R the code rate (set to 1/3), F the scaling factor (set to 1), N the maximum number of allocated resource blocks (set to 264 which corresponds to a subcarrier spacing of 120 kHz), T the symbol duration (calculated via $\frac{10^{-3}}{14 \cdot 2^{\mathrm{n}}}$ with n the numerology), and OH the overhead (set to 0.18 for frequency range 2 of the 5G specification) [45].

$$\mathrm{DR} = Q \cdot R \cdot F \cdot \frac{12N}{T} \cdot (1 - OH) \cdot 10^{-6} \tag{6}$$

In this equation, a SISO system with a single layer is considered, in order to compare with the IEEE Std. 802.11ad technology. The numerology for a subcarrier spacing of 120 kHz is n = 3, and the corresponding data rates range from 97 Mbps for BPSK up to 776 Mbps for 256-QAM for a channel bandwidth of 400 MHz.

At 60 GHz, IEEE Std. 802.11ad radios are considered, with channel bandwidths of 2.16 GHz and a single carrier physical layer. The data rates range from

375 375 Mbps for BPSK up to 4.62 Gbps for 16-QAM modulation which requires an SNR of 12.6 dB [10]. An orthogonal frequency division multiplexing (OFDM) physical layer is also available with higher data rates but is not considered for the remainder of this paper.

Currently, no wireless communication systems exist at 140 GHz. To compare future wireless communication systems at 140 GHz with existing technologies at 28 GHz and 60 GHz, the channel capacity for the three frequencies is analyzed, which is calculated via (7), with C the channel capacity in bits/s, B the channel bandwidth in Hz, and signal-to-noise ratio SNR.

$$\mathrm{C} = \mathrm{B}\log_2(1 + \mathrm{SNR}) \tag{7}$$

3. Network analysis

380 ### *3.1. Overview*

A summary of the averaged network metrics for the different scenarios is presented in Table 5, considering a single POP device and without considering EDGE devices. The average CPE vertex degree $\delta_{\mathrm{v,avg}}$ increases when more CPE devices are present in the network. For the same number of CPE devices, the
385 average CPE vertex degree decreases when more buildings are present, from 5.7 for a rural environment to 1.4 for a city center. The low POP eccentricity ϵ_{POP} for an urban city with few CPE devices (50 or 100) can be explained by the large number of unconnected CPE devices, i.e., the CPE devices for which no route towards the POP exists before adding EDGE devices. The vertex characteristics
390 of the POP device are critical to the success of the network deployment. The POP eccentricity is an important parameter for the latency, whereas the vertex degree influences the total network capacity, as all the FWA network traffic is carried over one of the edges of the POP node. The median link distance $\mathrm{d_{med}}$ gives an indication of the maximum throughput of the data that gets transmitted over
395 the wireless links. In the urban village pilot deployment or rural environment, the median path length is larger and the capacity of the links will be lower.

Table 5: FWA network characterization for different environments and network densities, with $\delta_{\text{v, avg}}$ the average CPE vertex degree, ϵ_{POP} the POP eccentricity, d_{med} the median link distance in meter, l_{avg} the average path length towards the POP in hop count, and c_{avg} the average percentage of connected CPE devices without adding any EDGE devices.

Environment	# CPE	$\delta_{\text{v, avg}}$	ϵ_{POP}	d_{med}	l_{avg}	c_{avg}
Urban city	50	1.43	1.40	77.80 m	1.18	3.6%
Urban city	100	2.10	2.12	80.45 m	1.50	2.9%
Urban city	300	3.48	6.36	78.46 m	3.43	5.7%
Urban city	600	4.63	14.72	77.37 m	7.19	23.8%
Urban village	50	2.39	4.14	136.3 m	2.15	31.5%
Urban village	100	3.35	8.24	116.7 m	3.37	65.3%
Urban village	300	7.30	6.94	106.1 m	3.22	97.5%
Urban village	600	12.86	6.02	99.2 m	3.36	98.8%
Rural	10	2.00	1.50	247.3 m	1.21	45.0%
Rural	50	5.68	4.50	214.6 m	2.10	86.4%

In an urban city, median link distances are limited to 80 m, irrespective of the number of CPE devices, as buildings obstruct links with a larger distance.

Analyzing the average percentage of connected CPE devices, i.e., the devices for which a path towards the POP exists irrespective of the link capacity, reveals that a single POP is not sufficient for a city environment. EDGE devices are critical for the FWA network deployment in urban cities. Adding EDGE devices is required in the field trial or early adopter phase for the urban village and rural scenarios, but with a sufficient number of network subscribers, the average percentage of connected CPE devices exceeds 86%. The average link length increases as fewer buildings are present, ranging from 77 m for an urban city up to 247 m for a rural environment.

3.2. Link budget calculations

The metrics from Table 5 are based on the input graph, i.e., the number and location of CPE devices and the number and placement of buildings. Therefore, they do not depend on the used frequency band, weather conditions, or obstructions due to vegetation. Based on the channel models presented in Section 2.1, and using the link budget calculations from Section 2.2, the maximum data rate on each link can be calculated based on the distances between FWA devices.

We performed link budget calculations for mmWave 5G and IEEE Std. 802.11ad. The transmit power P_T is 10 dBm, and we consider no losses in the transmitting and receiving devices ($L_T = L_R = 0$ dB). In an FWA network, there is bidirectional communication between identical devices. Therefore, the antenna gains of the transmit and receive antennas are the same. The total equivalent isotropically radiated power (EIRP), i.e., the sum of the transmit power and antenna gain, is subject to (local) regulations [40]. For mmWave 5G at 28 GHz, an antenna gain of 20 dBi is considered, resulting in an EIRP of 30 dBm that can be achieved with the Anokiwave AWMF-0129 antenna system [46]. At 60 GHz, the antenna gain of 32 dBi results in an EIRP of 42 dBm, which corresponds to the EIRP of the Terragraph IEEE Std. 802.11ad platform, consisting of 288 antenna elements [17].

The received power levels P_R are obtained via (5), and converted into SNR by subtracting the thermal noise floor, calculated via (8), with NF the noise floor in dBm, B the bandwidth in Hz, T the temperature in Kelvin, and k Boltzmann's constant equal to $1.379{\cdot}10^{-23}$ W Hz^{-1} K^{-1}.

$$\mathrm{NF} = 10 \log_{10} \left(\frac{\mathrm{kTB}}{1\mathrm{mW}} \right) \tag{8}$$

Figure 3 shows the maximum link distance in meters as a function of throughput for mmWave 5G and IEEE Std. 802.11ad technologies, considering a Line-of-Sight scenario and scenarios with two rain intensities. Even though the atmospheric loss and free space path loss are higher at 60 GHz, larger data rates are obtained for link distances up to 500 m as the channel bandwidths at 60 GHz are larger.

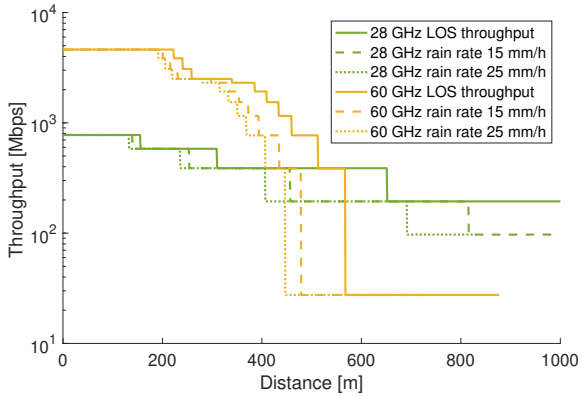

Figure 3: Maximum throughput as a function of distance for outdoor wireless networks at 28 GHz and 60 GHz.

3.3. Network capacity

Figure 4 shows the total network capacity, i.e., the sum of the link capacities of all wireless links in the network calculated via (7), as a function of the number of CPE devices, for different simulation configurations and averaged over the 50 simulations, for frequencies 60 GHz and 140 GHz. Table 6 presents the user requirements for the two considered use cases from Table 4. For use case 2, with different users requiring different data rates, the total user data rate requirement is lower than for use case 1, where all subscribers request 300 Mbps.

The total network capacity increase with an increasing number of CPE devices. The total capacity of the FWA network is higher using a carrier frequency of 140 GHz, assuming channel bandwidths of 4 GHz, compared to 60 GHz, with

Table 6: Total user data rate requirement for two use cases as a function of number of CPE devices.

Use case	10 CPE	50 CPE	100 CPE	300 CPE	600 CPE
1	3 Gbps	15 Gbps	30 Gbps	90 Gbps	180 Gbps
2	1.8 Gbps	9.0 Gbps	17.9 Gbps	53.7 Gbps	107.4 Gbps

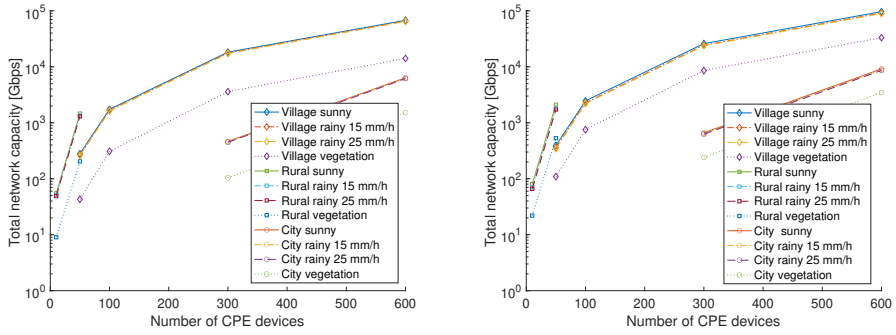

(a) 60 GHz (b) 140 GHz

Figure 4: Averaged total network capacity as a function of the number of customer premises equipment (CPE) devices.

2 GHz channel bandwidths. However, the curves in the two figures from Fig. 4 follow the same trends. For an urban city environment (represented by the circle symbols), the rain influence is limited which is due to the smaller link distances. However, the total network capacity lowers by 66% for 60 GHz and 53% for 140 GHz when 10% of the links are covered by vegetation. Due to the higher average CPE vertex degree, the network capacity is higher for an urban village.

Table 7 presents the influence of rain on the total available network capacity and average edge throughput that is available on the links for two environment scenarios, considering the IEEE Std. 802.11ad at 60 GHz, and comparing sunny weather with no additional attenuation to heavy rainfall with a specific attenuation of 10 dB/km. An early adopter scenario (with 100 CPE devices) is compared with a late majority scenario with 600 CPE devices. Investigation of the path loss for the different wireless links shows that additional attenuation due to rain does not seem to be substantial, as the average link distances are small. The additional attenuation ranges from 0.1 dB for the smaller links up to 3.7 dB for a link with a distance of 370 m. However, an additional attenuation of 3 dB has a considerable impact on the throughput that is available, as the receiver sensitivities for different MCS indices are close to one another [10].

Table 7: Influence of rain attenuation on total and average network throughput of an IEEE Std 802.11ad system at 60 GHz.

Scenario	Weather	Total throughput	AVG edge throughput
100 CPEs	Sun	411.940 Gbps	3.349 Gbps
100 CPEs	Rain rate 25 mm/h	360.500 Gbps	2.930 Gbps
600 CPEs	Sun	13 386.844 Gbps	3.502 Gbps
600 CPEs	Rain rate 25 mm/h	12 326.428 Gbps	3.225 Gbps

For the early adopter scenario, the total network throughput, i.e., the sum of the throughputs of all wireless links, decreases by 12.5% and the average edge throughput decreases by 419 Mbps in the event of heavy rain. For the late majority scenario, the total network throughput decreases by 8% and the average edge throughput decreases by 277 Mbps. We conclude that the impact of rain on the late majority scenario is lower than for the early adopter scenario. This is caused by the smaller link distances for a denser scenario.

4. Network planning

The goal of the network routing algorithm is to define a route from each CPE towards the POP, given a predefined quality of service (QoS) requirement, i.e., a certain throughput needs to be allocated on the edges from a CPE device to the POP device.

For the validation of the network planning algorithm, an IEEE Std. 802.11ad wireless system is considered, with a carrier frequency of 60 GHz and data rates up to 4.6 Gbps for a single-carrier physical layer (PHY). Furthermore, we assume that the required maximum download speed is 300 Mbps for each CPE, which corresponds to twice the typical download speed of a Belgian telecom operator [47].

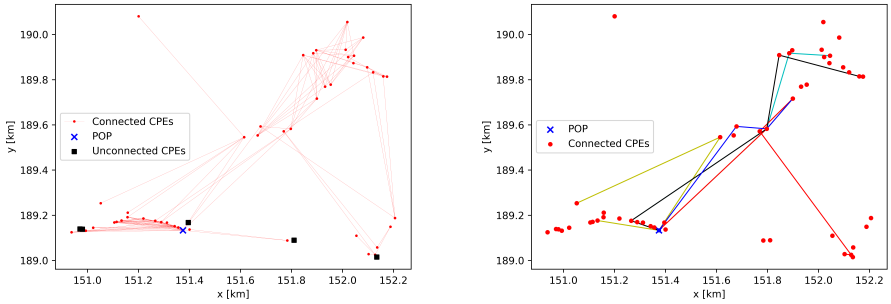

(a) Graph representation

(b) Network planning

Figure 5: Graph representation and planning of a simulation in rural environment with 50 CPE devices, with the edge colors in Fig. 5b representing the paths from some CPE devices towards the POP device.

4.1. Network planning rural environment

The rural environment from Fig. 2c is considered, with 50 CPE devices randomly distributed on the floor map. The graph representation of a single simulation result is shown in Fig. 5a and has the following metrics. The average CPE vertex degree is 5.26, the POP eccentricity is 5.0, the median link distance is 199.7 m, and the average number of hops towards the POP is 2.3.

The input graph is not connected, as 4 CPE devices do not have a link to another device. These CPE devices are represented by a black square in Fig. 5a, and an analysis of Fig. 2c shows that they will be able to connect to neighboring devices if they are located at another facade of the same building. In ideal scenarios, i.e., no rain and no vegetation obstructing the LOS paths, all links have a throughput of 4.62 Gbps. This is in line with Fig. 3, as the maximum link distance is less than 600 m. The sum of all user data rate requirements for use case 1, i.e., all user request 300 Mbps, is 15 Gbps, whereas the sum of all throughputs on the links to the POP is 73.92 Gbps. When it is raining with a rain rate of 25 mm/h, it is not possible to use the maximum data rate on all links (the maximum throughput of links exceeding 600 m decreases to 2.5 Gbps), and the

sum of all throughputs towards the POP decreases to 67.374 Gbps. Therefore, the links towards the POP have enough capacity to transfer the data of all CPEs. When 10% of the links are obstructed by vegetation, the available data rates decrease significantly, making communication impossible on most links. Only for link distances below 130 m is a data rate of at least 385 Mbps possible. For this scenario, the sum of the throughputs on the links towards the POP is 8.33 Gbps which is not sufficient to carry all aggregated user data. Even when only 5% of all links are covered by vegetation, there is a capacity bottleneck on the links towards the POP, with an available throughput of 11.659 Gbps.

For defining the path from each CPE device towards the single POP device, the CPE devices are first sorted. All devices have a throughput requirement of 300 Mbps and 80% of all devices have a single shortest path towards the POP. These devices are sorted based on the hop count on the shortest path, and network planning is performed first for the CPE devices with the largest hop count. For the scenario without any vegetation present, all CPE devices have a path towards the POP. Some examples are presented in Fig. 5b, in which the red lines indicate the path with the largest hop count.

4.2. Network planning urban village environment

Running the network planning algorithm using the urban village simulation data with 100 CPE devices results in a first warning that 16 CPE devices are not in the same cluster as the POP: 8 CPE devices do not have any connection and 2 clusters of respectively 5 and 3 CPE devices are interconnected but not connected to the main cluster. From the graph visualization in Fig. 6a and the floor map of the environment in Fig. 2b, it is clear that these devices can easily get connected by adding a limited number of EDGE nodes to the FWA network. In Fig. 6b, two EDGE devices are added at coordinates (153.668, 191.639) and (153.925, 191.800) that correspond to road intersections. Using this adjusted network, the network planning framework successfully performs network planning for the first 49 CPE devices before another warning is shown. From Fig. 6 it is clear that the number of links from the POP going North is limited, and this causes

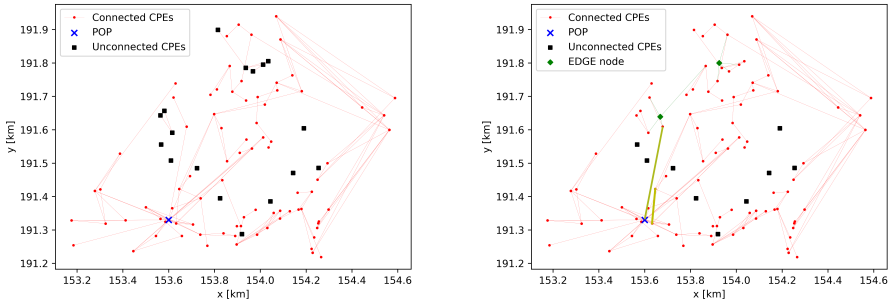

(a) Graph representation

(b) Two EDGE nodes added

Figure 6: Graph representation of a simulation in urban village environment with 100 CPE devices.

capacity constraints on the links that are plotted in yellow in Fig. 6b. To resolve the capacity constraint, EDGE devices can be added near coordinates (153.960, 191.560) and (153.660, 191.500). These EDGE devices create additional paths from the CPE devices in the North region towards the POP device. Another possibility is to investigate the placement of an additional POP device in the North region of Leest.

4.3. Discussion

The CPE devices have a small number of shortest paths to the POP device, and the number of hops on the shortest path is limited. The large bandwidths in the mmWave frequency band realize wireless networks where enough capacity is available on the wireless links to serve all users with a data rate that exceeds the data rate of current wired access networks. For an urban village and rural scenario, up to 5 EDGE devices need to be added to make the graph connected, i.e., to enable a connection from each CPE device to the POP device. For an urban city environment, more POP devices are required to get the CPE devices connected to the FWA network. Taking into account a vegetation map, i.e., with an indication of where trees are located, will allow a more realistic link

capacity calculation.

The optimal solution for the network routing of internet protocol data is the Busacker-Gowen algorithm which is an algorithm to solve minimum cost maximum flow problems [48]. In the Busacker-Gowen algorithm, data is routed from a user towards a server via multiple paths. The benefit of the proposed network planning algorithm compared to the Busacker-Gowen algorithm is that data is not split between multiple paths, i.e., all data from a certain CPE device follows the same path, even for multiple subscribers with different data rate requirements. This makes our implementation more suited for the planning of real FWA networks. In the current implementation, no beam steering loss and beam switching are considered, i.e., the angles of arrival and departure of the different links are not taken into account.

Compared to the FWA network planner of [49], where the CPE devices have no routing capabilities, very limited EDGE devices are required to enable network routing from all CPE devices towards the POP device. The CPE devices have routing capabilities, making the RF and networking architecture more complex, and therefore more expensive compared to CPE devices that only need a single wireless connection towards an EDGE device. In [49], 116 EDGE devices are required to cover 100 CPE devices (without routing capabilities) in the urban village of Leest, and therefore, the total installation cost of the CPE and EDGE devices for a telecom operator will be lower using our proposed network architecture.

5. Conclusions

In this paper, we have used graph theory to analyze the architecture of FWA networks adopting realistic channel models for performing reliable link budget calculations. Furthermore, we presented a routing algorithm to define how CPE devices can route their internet data traffic towards the POP device that connects to the wired infrastructure.

Some graph metrics, including the average vertex degree and the average

path length, influence the capacity of the network, e.g., what the average available link throughput is, whereas other metrics, e.g., the average hop count, influence wireless system characteristics such as latency. An example of the latter is the average hop count which is related to the packet latency. Due to the high vegetation loss at mmWave frequencies, capacity bottlenecks occur when even a small part of the link, i.e., 5% or 10%, is obstructed by vegetation. Due to the short link distances, the rain attenuation does not have a considerable effect. The larger bandwidths that are available at higher frequencies, 400 MHz at 28 GHz versus 2.16 GHz at 60 GHz, enable larger data rates. The influence of the high atmospheric loss at 60 GHz is limited due to the small link distances.

For the validation of the proposed network planning algorithm, an example is provided to perform FWA network planning using IEEE Std. 802.11ad technology operational in the 60 GHz band. The network planning determines the route from each CPE device towards the POP device, considering the channel capacities of the wireless links. When certain CPE are not connected to the network or the available capacity is not sufficient, EDGE devices need to be added to the network. The EDGE devices act as a router and do not connect customers directly. For urban city environments, the EDGE devices are critical to get CPE devices connected to the network. In this work, the placement of EDGE devices is considered to be a manual task that is performed by the network operator. Based on the location where the capacity bottleneck occurs, and based on the local regulations, the operator adds EDGE devices to increase the capacity. It was shown that a limited number of EDGE devices is sufficient for rural and urban village scenarios.

In the current work, a constant antenna gain is considered for all beam forming angles. Future work includes analyzing beam steering loss and realistic antenna beam patterns for CPE devices that maintain multiple links. Also, non-Line-of-Sight links can be considered, e.g., by searching for paths with a single building reflection and using typical reflection loss values from the literature. On higher layers, scheduling and medium access control mechanisms need to be investigated.

Appendix: network modeling and planning framework

The framework for FWA network characterization and network planning is implemented in Python and has been made available on GitHub: https://github.com/brdb/fwa-network-modeling-and-planning. In this appendix, a brief overview of the code structure is provided. For a detailed presentation, we refer to the README.md file in the repository. The repository has the following file structure.

```
/
├── README.md: general overview
├── docs: documentation
├── core
│   ├── graph_analysis.py: analyze network characteristics based on
│   │   graph
│   ├── graph_creation.py: create a graph based on input data
│   ├── graph_extension.py: extend graph by adding EDGE devices
│   ├── graph_preparation.py: perform link budget calculations
│   └── network_planning.py: run network planning algorithm
├── utils: helper functions used by the functions in core
│   ├── util_graph.py: helper for graph operations, including plotting
│   │   functionality
│   ├── util_linkbudget.py: helper for link budget calculations
│   └── util_planning.py: planning algorithm
├── data: input data generated with the GRAND tool
│   ├── environments: floor map for three environments
│   ├── UC1_100CPE_UrbanVillage: generated data from 50 simulations
│   ├── ...
│   ├── UC3_600CPE_UrbanCity: generated data from 50 simulations
│   └── README.md: description of data acquisition and file formats
├── examples: example scripts used to acquire the data presented
│   in this paper
├── scripts: MATLAB scripts to visualize the data and results
│   ├── visualize_capacity_analysis.m
│   ├── visualize_required_capacity.m
│   └── visualize_environment_map.m
├── results
└── test
    ├── sanity_check_igraph_metrics.py: validation iGraph package
    ├── test_analysis.py
    ├── test_graph_analysis.py
    └── test_routing.py
```

The simulation data from the GRAND tool, discussed in Section 2.5, for 50 simulations can be found in the `data` directory for the different scenarios discussed in this paper (Table 3). In the file `graph_creation` from the `core` directory, the input data is parsed and a graph is constructed, using the Python *iGraph* package. The vertices represent CPE devices, and the edges represent Line-of-Sight links between the devices. In the file `graph_extension`, the file with EDGE device locations and links is parsed and the EDGE devices are added to the graph. The characterization of an input graph, presented in Section 3.1, is performed via the file `graph_analysis`. The file `network_planning` implements the network planning algorithm from Section 2.4. Helper functions for the visualization of graphs and for the link budget calculations to transform the link distance into available throughputs and link capacities are present in the `utils` directory. In the `examples` directory, scripts are presented for the analysis and network planning of different scenarios, as an example how to use the presented framework. The script `graph_analysis_overview` generates the data from Table 5. The data from Fig. 4 is generated via `network_capacity_overview`, and the data from Table 7 is generated via `rain_influence_analysis`. The scripts used to illustrate the network planning algorithm are `UC1_network_planning_100CPE_UrbanVillage` and `UC1_network_planning_50CPE_Rural`. The `scripts` directory contains MATLAB scripts that are used for the visualization of the results, and to create the figures presented in this paper. The data from Table 4 is generated from the MATLAB script `visualize_required_capacity`. The Python scripts print relevant information to the console terminal, whereas debugging information is written to a `.log` file.

The framework also contains an implementation of graph simplification, by combining connected vertices into cliques and perform network planning for cliques, rather than individual CPE devices. However, this strategy introduces additional bottlenecks, i.e., there might be a bottleneck to route aggregated data from 3 CPE devices (e.g., 3×300 Mbps) to the POP device whereas 3 routes with 300 Mbps exist. As this strategy is sub-optimal, it is not presented in this paper.

Acknowledgement

This work was executed within the IMEC DBARC research project.

References

[1] Cisco annual internet report (2018–2023) white paper (August 2022).
URL https://www.cisco.com/c/en/us/solutions/collateral/executive-perspectives/annual-internet-report/white-paper-c11-741490.html

[2] K. J. Kerpez, R. Kinney, Integrated dsl test, analysis, and operations, IEEE Transactions on Instrumentation and Measurement 57 (4) (2008) 770–780. doi:10.1109/TIM.2007.910095.

[3] D. Nesset, Pon roadmap [invited], Journal of Optical Communications and Networking 9 (1) (2017) A71–A76. doi:10.1364/JOCN.9.000A71.

[4] N. Ioannou, D. Katsianis, D. Varoutas, Comparative techno-economic evaluation of lte fixed wireless access, fttdp g.fast and fttc vdsl network deployment for providing 30 mbps broadband services in rural areas, Telecommunications Policy 44 (3) (2020) 101875. doi:https://doi.org/10.1016/j.telpol.2019.101875.
URL https://www.sciencedirect.com/science/article/pii/S0308596118303860

[5] J. Du, D. Chizhik, R. Feick, M. Rodríguez, G. Castro, R. A. Valenzuela, Suburban fixed wireless access channel measurements and models at 28 ghz for 90% outdoor coverage, IEEE Transactions on Antennas and Propagation 68 (1) (2020) 411–420. doi:10.1109/TAP.2019.2935110.

[6] I. A. Alimi, R. K. Patel, N. J. Muga, A. N. Pinto, A. L. Teixeira, P. P. Monteiro, Towards enhanced mobile broadband communications: A tutorial on enabling technologies, design considerations, and prospects of 5g and beyond fixed wireless access networks, Applied Sciences 11 (21).

doi:10.3390/app112110427.
URL https://www.mdpi.com/2076-3417/11/21/10427

[7] Ieee standard for local and metropolitan area networks part 16: Air interface for broadband wireless access systems, IEEE Std 802.16-2009 (Revision of IEEE Std 802.16-2004) (2009) 1–2080doi:10.1109/IEEESTD.2009.5062485.

[8] I. A. Hemadeh, K. Satyanarayana, M. El-Hajjar, L. Hanzo, Millimeter-wave communications: Physical channel models, design considerations, antenna constructions, and link-budget, IEEE Communications Surveys Tutorials 20 (2) (2018) 870–913. doi:10.1109/COMST.2017.2783541.

[9] S. A. Busari, K. M. S. Huq, S. Mumtaz, L. Dai, J. Rodriguez, Millimeter-wave massive mimo communication for future wireless systems: A survey, IEEE Communications Surveys Tutorials 20 (2) (2018) 836–869. doi:10.1109/COMST.2017.2787460.

[10] IEEE 802.11ad - IEEE Standard for Information technology–Telecommunications and information exchange between systems–Local and metropolitan area networks–Specific requirements-Part 11: Wireless LAN Medium Access Control (MAC) and Physical Layer (PHY) Specifications Amendment 3: Enhancements for Very High Throughput in the 60 GHz Band, IEEE Computer Society, 2012.

[11] IEEE 802.11ay-2021 - IEEE Standard for Information Technology–Telecommunications and Information Exchange between Systems Local and Metropolitan Area Networks–Specific Requirements Part 11: Wireless LAN Medium Access Control (MAC) and Physical Layer (PHY) Specifications Amendment 2: Enhanced Throughput for Operation in License-exempt Bands above 45 GHz, IEEE Computer Society, 2021.

[12] S. Hurley, S. Allen, D. Ryan, R. Taplin, Modelling and planning fixed wireless networks, Wireless Networks 16 (3) (2010) 577–592. doi:10.1007/

s11276-008-0155-9.
URL https://doi.org/10.1007/s11276-008-0155-9

[13] O. Kaddoura, J. Outes-Carnero, J. A. Garcia-Fernandez, R. Acedo-Hernandez, M. Ceron-Larrubia, L. Rios, J. J. Sanchez-Sanchez, R. Barco, Greenfield design in 5g fwa networks, IEEE COMMUNICATIONS LETTERS 23 (12) (2019) 2422–2426. doi:10.1109/LCOMM.2019.2939470.

[14] J. Zhang, C. Masouros, Learning-based predictive transmitter-receiver beam alignment in millimeter wave fixed wireless access links, IEEE Transactions on Signal Processing 69 (2021) 3268–3282. doi:10.1109/TSP.2021.3076899.

[15] M. K. Adityo, M. I. Nashiruddin, M. A. Nugraha, 5g fixed wireless access network for urban residential market: A case of indonesia (2021) 123–128doi:10.1109/IoTaIS53735.2021.9628442.

[16] S. Nie, G. R. MacCartney, S. Sun, T. S. Rappaport, 28 ghz and 73 ghz signal outage study for millimeter wave cellular and backhaul communications, in: 2014 IEEE International Conference on Communications (ICC), 2014, pp. 4856–4861. doi:10.1109/ICC.2014.6884089.

[17] B. De Beelde, Z. Verboven, E. Tanghe, D. Plets, W. Joseph, Outdoor mmwave channel modeling for fixed wireless access at 60 ghz, Radio Science [submitted] (2022) 1–1.

[18] B. De Beelde, E. Tanghe, D. Plets, W. Joseph, Outdoor channel modeling at d-band frequencies for future fixed wireless access applications, IEEE Wireless Communications Letters (2022) 1–1doi:10.1109/LWC.2022.3202921.

[19] K. Aldubaikhy, W. Wu, N. Zhang, N. Cheng, X. Shen, mmwave ieee 802.11ay for 5g fixed wireless access, IEEE Wireless Communications 27 (2) (2020) 88–95. doi:10.1109/MWC.001.1900174.

[20] Z.-K. Weng, A. Kanno, P. T. Dat, K. Inagaki, K. Tanabe, E. Sasaki, T. Kürner, B. K. Jung, T. Kawanishi, Millimeter-wave and terahertz fixed wireless link budget evaluation for extreme weather conditions, IEEE Access 9 (2021) 163476–163491. doi:10.1109/ACCESS.2021.3132097.

[21] T. Schneider, A. Wiatrek, S. Preussler, M. Grigat, R.-P. Braun, Link budget analysis for terahertz fixed wireless links, IEEE Transactions on Terahertz Science and Technology 2 (2) (2012) 250–256. doi:10.1109/TTHZ.2011.2182118.

[22] G. R. MacCartney, M. K. Samimi, T. S. Rappaport, Omnidirectional path loss models in new york city at 28 ghz and 73 ghz, in: 2014 IEEE 25th Annual International Symposium on Personal, Indoor, and Mobile Radio Communication (PIMRC), 2014, pp. 227–231. doi:10.1109/PIMRC.2014.7136165.

[23] J. Dudzinsky, S. J., Atmospheric effects on terrestrial millimeter-wave communications, in: 4th European Microwave Conference, 1974, pp. 197–201.

[24] G. A. Siles, J. M. Riera, P. Garcia-del Pino, Atmospheric attenuation in wireless communication systems at millimeter and thz frequencies [wireless corner], IEEE Antennas and Propagation Magazine 57 (1) (2015) 48–61. doi:10.1109/MAP.2015.2401796.

[25] Attenuation by atmospheric gases and related effects, ITU-R P.676-12.

[26] J. Wells, Faster than fiber: The future of multi-g/s wireless, IEEE Microwave Magazine 10 (3) (2009) 104–112. doi:10.1109/MMM.2009.932081.

[27] O. Zahid, S. Salous, Long-term rain attenuation measurement for short-range mmwave fixed link using dsd and itu-r prediction models, Radio Science 57 (4) (2022) e2021RS007307, e2021RS007307 2021RS007307. arXiv:https://agupubs.onlinelibrary.wiley.com/doi/pdf/10.1029/2021RS007307, doi:https://doi.org/10.1029/2021RS007307.

URL https://agupubs.onlinelibrary.wiley.com/doi/abs/10.1029/2021RS007307

[28] Z. A. Shamsan, Rainfall and diffraction modeling for millimeter-wave wireless fixed systems, IEEE Access 8 (2020) 212961–212978. doi:10.1109/ACCESS.2020.3040624.

[29] B. De Beelde, D. Plets, E. Tanghe, C. Li, W. Joseph, V-band rain attenuation measurement setup, in: 2022 3rd URSI AT-AP-RASC, Gran Canaria, 29 May – 3 June 2022, 2022, pp. 1–4.

[30] ITU-R-P.838-3, Specific attenuation model for rain for use in prediction methods, Tech. rep., International Telecommunication Union (2005).

[31] M. A. Weissberger, An initial critical summary of models for predicting the attenuation of radio waves by trees, Final Report Electromagnetic Compatibility Analysis Center (Jul. 1982).

[32] I. R. C. Committee, Recommendations and Reports of the CCIR, 1986: Propagation in non-ionized media, Recommendations and Reports of the CCIR, 1986:, International Telecommunication Union, 1986.
URL https://books.google.be/books?id=P_AtAQAAIAAJ

[33] G. Dooren, van, H. Govaerts, M. Herben, COST 235: Radiowave propagation effects on next-generation fixed-services terrestrial telecommunications systems, Technische Universiteit Eindhoven, 1997.

[34] B. De Beelde, R. De Beelde, E. Tanghe, W. Joseph, Vegetation loss at d-band frequencies and new vegetation-dependent exponential decay model, IEEE Transactions on Antennas and Propagation.

[35] A. Lagrone, Propagation of vhf and uhf electromagnetic waves over a grove of trees in full leaf, IEEE Transactions on Antennas and Propagation 25 (6) (1977) 866–869. doi:10.1109/TAP.1977.1141708.

[36] M. Al-Nuaimi, R. Stephens, Measurements and prediction model optimisation for signal attenuation in vegetation media at centimetre wave frequencies, IEE Proceedings - Microwaves, Antennas and Propagation 145 (1998) 201–206(5).
URL https://digital-library.theiet.org/content/journals/10.1049/ip-map_19981883

[37] B. De Beelde, , D. Plets, W. Joseph, Characterization of vegetation loss and impact on network performance at v-band frequencies, IEEE Antennas and Wireless Propagation Letters [submitted] (2022) 1–1.

[38] Base station planning permission in europe, Tech. rep., GSM Association (2013).
URL https://www.gsma.com/publicpolicy/wp-content/uploads/2013/05/GSMA_BaseStation_Planning_EuropeWEB.pdf

[39] M. van Steen, Graph Theory and Complex Networks: An Introduction, Maarten van Steen, 2010.
URL https://books.google.be/books?id=V7bMbwAACAAJ

[40] E. Commission, C/2020/4872: Commission implementing regulation (eu) 2020/1070 of 20 july 2020 on specifying the characteristics of small-area wireless access points pursuant to article 57 paragraph 2 of directive (eu) 2018/1972 of the european parliament and the council establishing the european electronic communications code, Official Journal of the European Union.

[41] M. Deruyck, E. Tanghe, D. Plets, L. Martens, W. Joseph, Optimizing LTE wireless access networks towards power consumption and electromagnetic exposure of human beings, COMPUTER NETWORKS 94 (2016) 29–40.
URL http://dx.doi.org/10.1016/j.comnet.2015.11.023

[42] G. Castellanos, S. De Gheselle, L. Martens, N. Kuster, W. Joseph, M. Deruyck, S. Kuehn, Multi-objective optimisation of human exposure

for various 5g network topologies in switzerland, Computer Networks 216 (2022) 109255. doi:https://doi.org/10.1016/j.comnet.2022.109255.
URL https://www.sciencedirect.com/science/article/pii/S1389128622003231

[43] OpenStreetMap contributors, Planet dump retrieved from https://planet.osm.org , https://www.openstreetmap.org (2017).

[44] T. Tuovinen, N. Tervo, A. Pärssinen, Analyzing 5g rf system performance and relation to link budget for directive mimo, IEEE Transactions on Antennas and Propagation 65 (12) (2017) 6636–6645. doi:10.1109/TAP.2017.2756848.

[45] 3rd Generation Partnership Project, New radio; user equipment (ue) radio access capabilities (2020).

[46] Awmf-0129: Single pol 64-element mmw active antenna innovator's kit (2022).
URL https://www.anokiwave.com/products/awmf-0129/index.html

[47] Telenet one subscription plan (202).

[48] M. Fu, Z. Zheng, Y. Zhuang, B. Quan, Z. Le, A busacker–gowen algorithm based on routing scheme for maximizing throughput with minimum delay in woban, in: S. Xing, S. Chen, Z. Wei, J. Xia (Eds.), Unifying Electrical Engineering and Electronics Engineering, Springer New York, New York, NY, 2014, pp. 1593–1601.

[49] G. Castellanos, B. De Beelde, D. Plets, L. Martens, W. Joseph, M. Deruyck, Evaluating 60 ghz fwa deployments for urban and rural environments in belgium., Computer Networks.